Catal Lett (2008) 123:150–155
DOI 10.1007/s10562-008-9409-5

Catalytic Performance of Activated Carbon Supported Tungsten Carbide for Hydrazine Decomposition

Jun Sun · Mingyuan Zheng · Xiaodong Wang · Aiqin Wang · Ruihua Cheng · Tao Li · Tao Zhang

Received: 1 November 2007 / Accepted: 22 January 2008 / Published online: 5 February 2008

Abstract Activated carbon (AC) supported tungsten carbide was reported for the catalytic decomposition of hydrazine for the first time. It was found that the WC_x/AC-H catalyst prepared by a carbothermal hydrogen reduction process exhibited excellent catalytic performances both in the microreactor and in a 1 Newton hydrazine microthruster. The XRD, TEM and microcalorimetry results suggest that the formation of well crystallized W_2C phase, the restraining of the carbon deposition, as well as the prohibiting of the methanation should be responsible for the high activity and stability of the WC_x/AC-H catalyst in the hydrazine decomposition reaction.

Keywords Hydrazine decomposition · Activated carbon · Tungsten carbide · Deposited carbon · Microcalorimetry · Microthruster

1 Introduction

Catalytic decomposition of hydrazine in microthrusters has been widely applied to attitude control of spacecrafts and satellites. The commercial catalyst for this reaction is Ir/Al_2O_3 with a very high loading of the iridium (20–40%) [1, 2]. However, the high cost and limited resources of the iridium has stimulated much interest to search for new cheaper alternative catalysts for hydrazine decomposition.

J. Sun · M. Zheng · X. Wang · A. Wang · R. Cheng · T. Li · T. Zhang (✉)
State Key Laboratory of Catalysis, Dalian Institute of Chemical Physics, CAS, Dalian 116023, P.R. China
e-mail: taozhang@dicp.ac.cn

J. Sun
Graduate School of the Chinese Academy of Sciences, Beijing 100049, China

It has been well established that transition metal nitrides, carbides, and phosphides exhibited good catalytic performances in hydrogen-involving reactions, even comparable to the noble metals [3–5]. In the past decade, we [6–11] and other groups [12–14] tested this type of intermetallic compounds in the catalytic decomposition of hydrazine, and found that they exhibited high catalytic activities for the hydrazine decomposition. These results suggested that the transition metal nitrides, carbides, and phosphides have the potential to substitute the expensive Ir/Al_2O_3 catalyst. In our previous studies, active component, such as Mo_2C [6], MoN_x [8], and MoP [11], was supported on the commercial alumina in order to obtain the desired mechanical strength. Compared with alumina supports, activated carbon has been little used as the support for hydrazine decomposition, in spite of its large surface area and well developed porosity. The underlying reason may lie in that the activated carbon tends to react with H_2 (one of the products of hydrazine decomposition) through methanation reaction, which would be a pronounced side reaction at high temperatures. Recently, Vieira et al. reported that carbon nanofibers with macroscopic shaping could act as an interesting support of iridium for hydrazine decomposition [15–17], but they did not report the methanation side effect. To the best of our knowledge, tungsten carbide supported on activated carbon has so far not been attempted for N_2H_4 decomposition, although it could be prepared under relatively mild conditions via a carbothermal reduction or carbothermal hydrogen reduction process [18]. In the present work, we for the first time reported that the activated carbon supporting tungsten carbide (W_2C/AC) exhibited excellent performance in the hydrazine decomposition, which was superior to the alumina supporting one (WC/Al_2O_3). More intriguing, methanation was negligible on the W_2C/AC, while it was remarkable on the Ir/AC.

2 Experiments

2.1 Catalyst Preparation

The preparation of tungsten carbide on activated carbon support is similar to that reported by Liang et al. [18]. An aqueous solution of ammonium metatungstate containing desired W content was impregnated onto the activated carbon (provided by NORIT Company, with a specific area of 1280 m^2/g) or alumina (home-made, with a specific area of 217 m^2/g) support, followed by drying at 120 °C overnight and calcination at 500 °C in N_2 (for AC) or in air (for Al_2O_3) for 3 h to obtain WO_3/AC and WO_3/Al_2O_3. Subsequently, the WO_3/AC was carburized in H_2 with the following heating ramp: from room temperature to 450 °C in 40 min, then to 850 °C at a rate of 1 °C/min and kept at 850 °C for 1 h. The resultant sample is denoted as WC_x/AC-H. For comparison, bulk WC, WC_x/AC-CH and WC_x/Al_2O_3-CH were prepared by treating WO_3, WO_3/AC and WO_3/Al_2O_3 in a CH_4/H_2 (20 vol% CH_4) mixture atmosphere with the same heating program. In addition, Ir/AC and Ir/Al_2O_3 were also prepared by impregnating the support with an aqueous solution of H_2IrCl_6, and then drying at 120 °C for 12 h and calcining at 350 °C for 4 h, and finally reducing in H_2 for 2 h. The tungsten and iridium loadings of the catalysts are varied with the supports and the catalytic tests, as shown in Table 1.

2.2 Catalyst Characterization

X-ray diffraction (XRD) patterns of the samples were obtained with an X′pert (PANalytical) diffractometer operated at 40 kV and 100 mA, using Ni-filtered Cu-Kα radiation. Transmission electron microscopy (TEM) analyses were performed on a JEM-2000EX (JEOL) microscope. Microcalorimetry of CO adsorption was performed at 40 °C using a Calvet-type microcalorimeter (Setaram BT 2.15) as described in detail elsewhere [11, 19].

2.3 Microreaction Tests

The catalysts were evaluated at atmospheric pressure in a fixed-bed reactor [9–11]. A catalyst sample (50 mg for a supported catalyst and 40 mg for an unsupported catalyst) was diluted with silica and loaded in a U-shaped quartz microreactor. Before reaction, the catalyst was pre-reduced with the corresponding carburizing gas at 850 °C for 0.5 h. Then, the feed gas containing 3 vol% N_2H_4 in Ar, which was obtained by bubbling liquid N_2H_4 at 30 °C with Ar, was introduced to the reactor at a flow rate of 85 mL/min. The reaction temperature ranged from 30 °C to 700 °C. The effluent gas, containing the unconverted N_2H_4 and the products H_2, N_2, and NH_3, was analyzed using an on-line chromatograph (Agilent 6890) equipped with a thermal conductivity detector (TCD).

2.4 Bench-scale Tests

The bench-scale tests for hydrazine decomposition were performed with our specially designed reactor system [6, 8]. The catalysts used for bench-scale tests are of columned shape, around 1.5 mm in length and 1 mm in diameter. For each test, about 0.67 g of activated carbon supported catalyst or 0.90 g of alumina supported catalyst were loaded in a 1 Newton microthruster (30 mm in length and 7 mm in diameter). Considering the density difference between AC and Al_2O_3, loadings (W or Ir wt%) of 33.3% for AC supported catalysts while 24.8% for alumina supported catalysts were employed to ensure the same mass of active components in the catalyst bed of the microthruster. The injection of hydrazine was realized by pressurized N_2 at 0.8 MPa and the hydrazine feeding rate was kept at 0.49 g/s. The feeding of hydrazine was controlled by an electromagnetic valve. Before ignition, the catalyst bed was preheated to a specified temperature (T_i). The parameters, including catalyst bed temperature (T_c), chamber pressure (P_c), and ignition delay (t_{90}), were measured and recorded with a computer, and they are regarded as indexes for catalyst performances.

3 Results and Discussion

3.1 Characterization of the Catalysts

In this work, a carbothermal hydrogen reduction [18] and a temperature-programmed reaction (CH_4/H_2-TPR) [20] were respectively employed for preparing tungsten carbides on the activated carbon and alumina supports, and the crystalline phases formed were examined with XRD. As shown in Fig. 1, the WC_x/AC-H which was prepared

Table 1 Metal loadings of the catalysts used for microreactor and microthruster tests

Catalysts	WC_x/AC-H	WC_x/AC-CH	Ir/AC	WC_x/Al_2O_3-CH	Ir/Al_2O_3
Tested in microreactor	16.7%	16.7%	–	16.7%	–
Tested in microthruster	33.3%	33.3%	33.3%	24.8%	24.8%

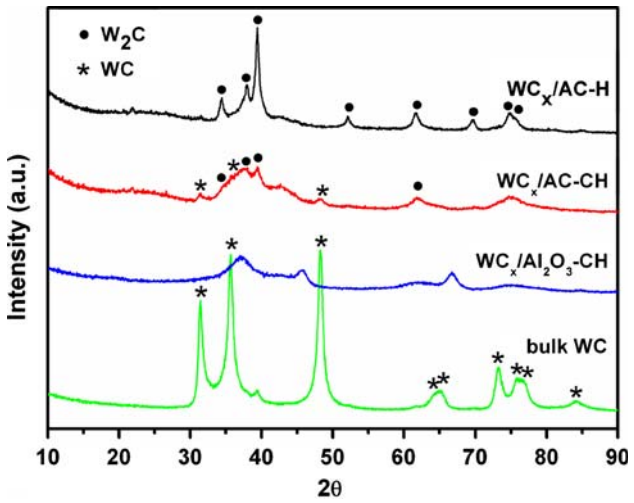

Fig. 1 XRD patterns of 16.7% WC_x/AC-H, 16.7% WC_x/AC-CH, 16.7% WC_x /Al_2O_3-CH and bulk WC

by the carbothermal hydrogen reduction route presents diffraction peaks typical for W_2C phase. According to [18], the formation of WC or W_2C was closely related with the carburizing temperature. When the carburizing temperature was higher than 850 °C, a mixture phase of WC and W_2C would be formed; whereas WO_x, W or their mixture would be formed at temperatures lower than 850 °C. On the other hand, when the CH_4/H_2-TPR route was employed, a mixture phase of WC and W_2C was formed at 850 °C, as identified by XRD on the WC_x/AC-CH sample. This result suggests that the CH_4/H_2-TPR may facilitate the carburization of W, but it usually causes contamination of carbide surface by polymeric carbon and covering of active sites [18], as we will demonstrate in the following part. Moreover, comparing the XRD patterns of the WC_x/AC-H and the WC_x/AC-CH, one can clearly see that the diffraction peaks of the WC_x/AC-CH are poorly revolved and the peak broadening seems to be more prominent, implying that the WC_x particle size on the WC_x/AC-CH is smaller than that on the WC_x/AC-H. It is noted that no any crystalline phase corresponding to WC or W_2C was detected by XRD on the WC_x/Al_2O_3-CH catalyst, although it was reported that WC was mainly formed on the Al_2O_3 support by this CH_4/H_2-TPR route [21]. This result suggests that the WC_x phase on the alumina support should be in a highly dispersed state.

To further examine the crystal size of the WC_x, TEM observations were performed on the above three supported catalyst samples. In well agreement with the XRD result, the WC_x/Al_2O_3-CH showed the smallest particles with sizes less than 2 nm (Fig. 2a), whereas the particle sizes on the WC_x/AC-CH were around 4–8 nm (Fig. 2b). On the contrary, the particles on the WC_x/AC-H were not uniform, spanning from several nanometers to tens of nanometers (Fig. 2c). According to the TEM results, the dispersion of the tungsten carbide follows the order of: WC_x/Al_2O_3-CH > WC_x/AC-CH > WC_x/AC-H, and this is also in accordance with the XRD results.

CO adsorption on the three catalysts was measured by microcalorimetry. As shown in Fig. 3a and Table 2, the WC_x/Al_2O_3-CH had the highest CO uptake (44.9 μmol/g), which was in accordance with the high dispersion of WC_x on the alumina support. It is surprising that the CO uptake on the WC_x/AC-H was the same as that on the WC_x/AC-CH, though the former catalyst had a much lower dispersion as visualized by the TEM image. The possible reason may be that carbon deposition occurred on the WC_x/AC-CH surface during the CH_4/H_2-TPR process, leading to a partial covering of the active sites. On the other hand, the WC_x/AC-H was prepared by the carbothermal hydrogen reduction process, and thus avoided the carbon deposition and blocking of the active sites. Figure 3b illustrates the differential heat for CO adsorption as a function of the CO coverage, which reflects the strength and distribution of the active sites on the catalyst surface. It can be seen that the WC_x/AC-H adsorbed CO molecules the most strongly among the three samples, suggesting that W_2C on the WC_x/AC-H was more active than the WC_x phase on the other two catalysts.

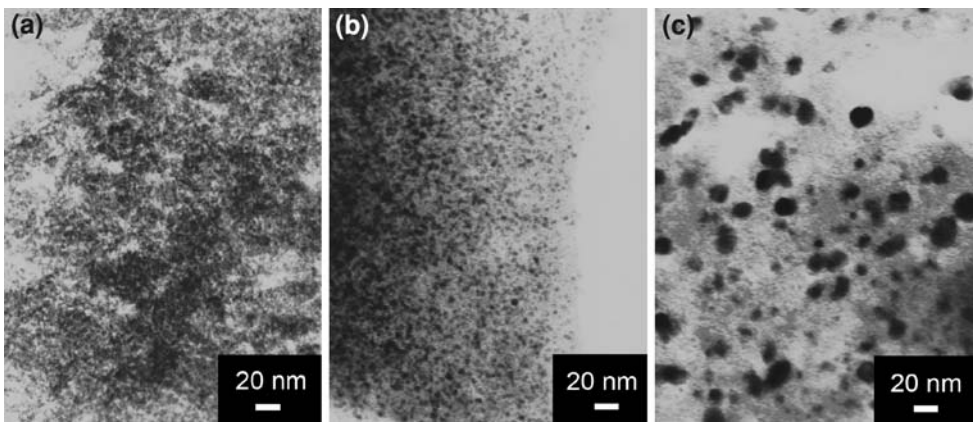

Fig. 2 TEM images of (**a**) 16.7% WC_x /Al_2O_3-CH, (**b**) 16.7% WC_x/AC-CH and (**c**) 16.7% WC_x/AC-H

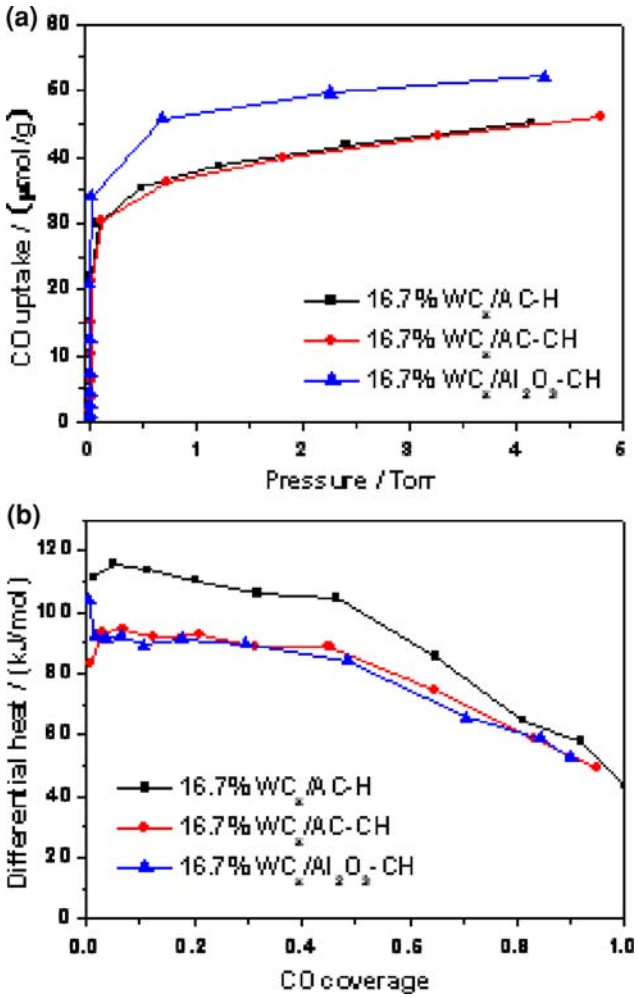

Fig. 3 (**a**) CO uptakes and (**b**) differential heats of CO adsorption over different catalysts

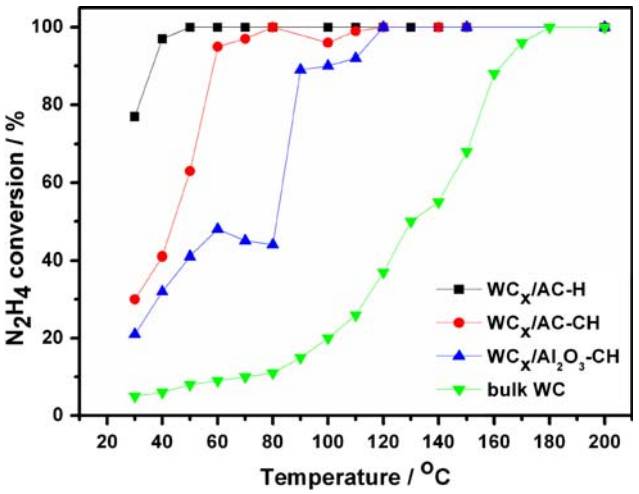

Fig. 4 Hydrazine conversions on 16.7% WC_x/AC-H, 16.7% WC_x/AC-CH, 16.7% WC_x/Al_2O_3-CH and bulk WC

3.2 Activities for Hydrazine Decomposition in a Microreactor

The three supported WC_x catalysts, as well as the bulk WC, were firstly evaluated in a microreactor for the hydrazine decomposition, and the results are illustrated in Fig. 4 and the turnover frequencies (TOFs) at 30 °C based on CO uptakes are calculated and listed in Table 2. Clearly, the N_2H_4 conversions on the three supported WC_x catalysts were much higher than that on the bulk WC, indicating dispersion of WC_x on the supports is necessary to obtain a high catalytic activity. Especially for the WC_x/AC-H catalyst, the hydrazine conversion attained 77% at 30 °C and 100% at 50 °C, which was significantly higher than those over the other catalysts. From Table 2, it can be seen that the TOF of N_2H_4 decomposition on the WC_x/AC-H is 0.764 s^{-1}, which is twice larger than that on the WC_x/AC-CH. According to the TOF values in Table 2, the activities of the four catalysts follow the order of WC_x/AC-H > WC_x/AC-CH > bulk WC > WC_x/Al_2O_3-CH. Evidently, the WC_x sites on the activated carbon are more active than those on the alumina, demonstrating the advantage of the activated carbon as the support for tungsten carbides. Moreover, on the activated carbon support, the W_2C sites resulting from the carbothermal hydrogen reduction behaved more actively than the WC_x sites obtained from the CH_4/H_2-TPR process. Interestingly, the TOF of bulk WC (0.188 s^{-1}) is higher than that of WC_x/Al_2O_3-CH, implying that the strong interaction between WC_x and Al_2O_3 makes the WC_x sites less active although it facilitates the dispersion of WC_x and increases the number of active sites.

3.3 Catalytic Performances Evaluated in a Microthruster

Since the WC_x/AC-H behaved best for the hydrazine decomposition in a microreactor, it was further evaluated in a 1 Newton hydrazine microthruster in comparison with

Table 2 The CO uptakes and TOFs of hydrazine decomposition on different catalysts

Catalysts	WC_x/AC-H	WC_x/AC-CH	WC_x/Al_2O_3-CH	Bulk WC
CO uptake (μmol/g)	35.6	35.7	44.9	9.4
TOF at 30 °C (s^{-1})	0.764	0.298	0.165	0.188

the Ir/Al_2O_3 catalyst, to probe its potential applications in propulsion systems. Before ignition, the temperature of the catalyst bed (T_i) was preheated to 160 °C. The microthrusters loaded with WC_x/AC-H, Ir/AC and Ir/Al_2O_3 started successfully, whereas the one loaded with WC_x/AC-CH started only when T_i was elevated to 180 °C. By contrast, the microthruster loaded with WC_x/Al_2O_3-CH failed to work with the T_i even higher than 200 °C. This result is consistent with that in the microreactor, reflecting the intrinsic activities of different catalysts.

Figure 5 compares the catalytic performances of the WC_x/AC-H and Ir/Al_2O_3 in the first 30 s continuous feeding of hydrazine with the T_i at 160 °C. Clearly, both the P_c curve and the T_c curve are very similar on the two catalysts, implying that the WC_x/AC-H has the potential to substitute the traditional Ir/Al_2O_3 catalyst. Table 3 summarizes the steady chamber pressure (P_c), steady catalyst bed temperature (T_c), and ignition delay (t_{90}) in the first 30 s continuous feeding of hydrazine on WC_x/AC-H, Ir/AC and Ir/Al_2O_3 with T_i at 160 °C. It can be seen that both P_c and T_c over the WC_x/AC-H were higher than those over the Ir/Al_2O_3, suggesting that the hydrazine decomposed more efficiently on the WC_x/AC-H catalyst. The ignition delay

Table 3 Results of hydrazine decomposition over different catalysts in the first 30 s continuous feeding of hydrazine with T_i at 160 °C

Catalysts	P_c (MPa)	T_c (°C)	t_{90} (ms)
24.8% Ir/Al_2O_3	0.462	682	460
33.3% Ir/AC	0.471	712	410
33.3% WC_x/AC-H	0.473	706	530

t_{90}, which reflected the initial activity of the catalysts, was slightly longer on the WC_x/AC-H than that on the two Ir-based catalysts, indicating that the initial activity of the WC_x/AC-H was comparable to the Ir-based catalysts. It is worthwhile to note that intensive oscillations and a sudden drop of the P_c occurred (Fig. 6a) when the Ir/AC was tested in the second 30 s continuous feeding of hydrazine. A weight loss of 62% was found for the Ir/AC after the test. However, a steady P_c curve could still be established over the WC_x/AC-H even in the tenth 30 s continuous feeding of hydrazine (Fig. 6b), and the weight loss after the test was only 6%. The great difference in the weight loss of the two catalysts suggests that methanation (between the carbon support and H_2 produced by N_2H_4 decomposition) occurred to a substantial degree during the reaction over

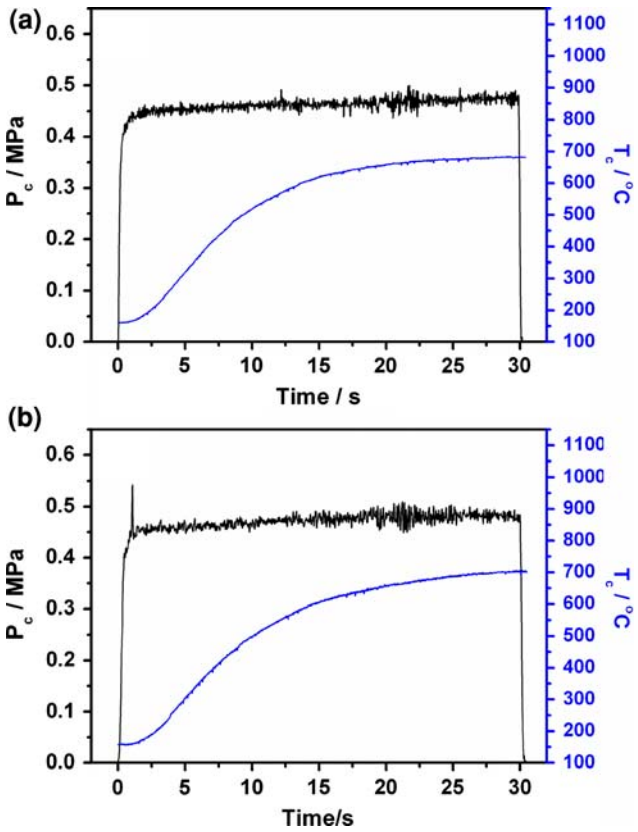

Fig. 5 Catalytic performances of (**a**) 24.8% Ir/Al_2O_3 and (**b**) 33.3% WC_x/AC-H catalysts in the first 30 s continuous feeding of hydrazine with T_i at 160 °C

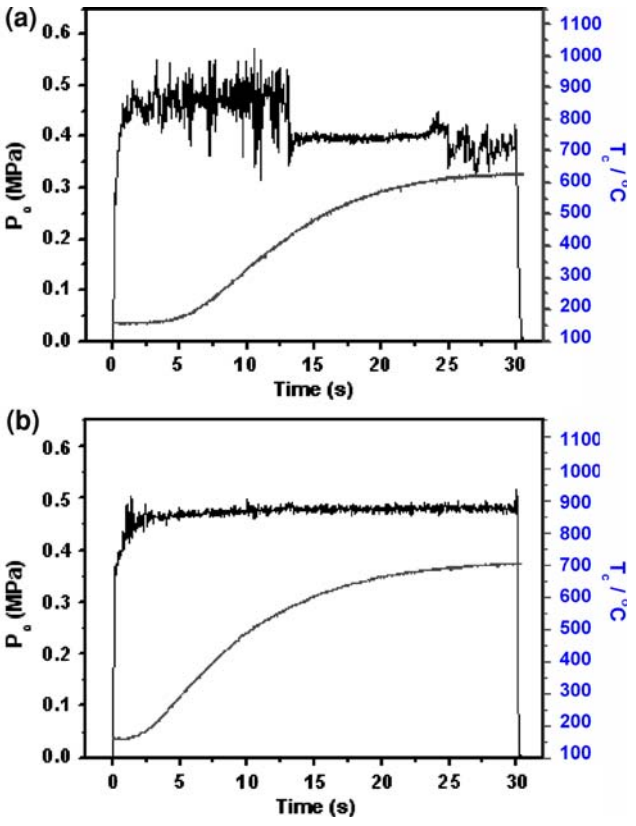

Fig. 6 Catalytic performances of (**a**) 33.3% Ir/AC in the second 30 s continuous feeding of hydrazine and (**b**) 33.3% WC_x/AC-H in the tenth 30 s continuous feeding of hydrazine with T_i at 160 °C

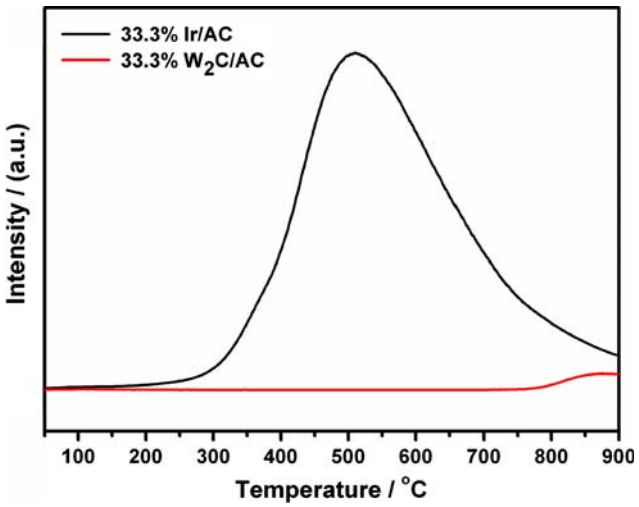

Fig. 7 CH_4 signals detected by mass spectrometry on the catalysts in TPSR in H_2 atmosphere

the activated carbon supported iridium catalyst. To confirm that, temperature-programmed surface reaction (TPSR) was performed in H_2 atmosphere. As shown in Fig. 7, CH_4 signal appeared apparently on the Ir/AC when the temperature was above 200 °C, and it reached maximum at 510 °C, which indicates that CH_4 can be easily formed on the Ir/AC catalyst under the promoting role of the noble metal iridium. On the contrary, CH_4 was detectable on the WC_x/AC-H only at above 800 °C. This result clearly demonstrated that the methanation reaction was negligible on the WC_x/AC-H catalyst, which rendered it as a highly efficient and stable catalyst for hydrazine decomposition.

4 Conclusion

Activated carbon supported tungsten carbides have been successfully used as the catalysts for hydrazine decomposition. It has been found that the WC_x/AC-H which was prepared by the carbothermal hydrogen reduction process exhibited the best catalytic performance both in the microreactor and in the microthruster. The formation of well crystallized W_2C phase, the restraining of the carbon deposition, as well as the prohibiting of the methanation, should be responsible for the high activity and stability of the WC_x/AC-H catalyst. By comparing with the traditional Ir/Al_2O_3, it was demonstrated that the WC_x/AC-H could be a promising substitute for the Ir-based catalyst for hydrazine decomposition in space technology.

Acknowledgments Financial supports of National Natural Science Foundation of China for Distinguished Young Scholars (No. 20325620) and National Natural Science Foundation of China (No. 20303017 and No. 20573108) are gratefully acknowledged.

References

1. Schmidt EW (2001) Hydrazine and its derivatives: preparation, properties, applications, 2nd edn. Wiley, New York, p 1267
2. U. S. Patent No 4,124,538
3. Levy RB, Boudart M (1973) Science 181:547
4. Oyama ST (1992) Catal Today 15:179
5. Chen JG (1996) Chem Rev 96:1477
6. Chen XW, Zhang T, Ying PL, Zheng MY, Wu WC, Xia LG, Li T, Wang XD, Li C (2002) Chem Commun 288
7. Chen XW, Zhang T, Zheng MY, Xia LG, Li T, Wu WC, Wang XD, Li C (2004) Ind Eng Chem Res 43:6040
8. Chen XW, Zhang T, Li C, Xia LG, Li T, Zheng MY, Wu ZL, Wang XD, Wei ZB, Xin Q (2002) Catal Lett 79:1
9. Chen XW, Zhang T, Zheng MY, Wu ZL, Wu WC, Li C (2004) J Catal 224:473
10. Zheng MY, Chen XW, Cheng RH, Li N, Sun J, Wang XD, Zhang T (2006) Catal Commun 7:187
11. Cheng RH, Shu YY, Zheng MY, Li L, Sun J, Wang XD, Zhang T (2007) J Catal 249:397
12. Rodrigues JAR, Cruz GM, Bugli G, Boudart M, Djéga-Mariadassou G (1997) Catal Lett 45:1
13. Brayner R, Djéga-Mariadassou G, Cruz GM, Rodrigues JAJ (2000) Catalysis Today 57:225
14. Santos JBO, Valenca GP, Rodrigues JAJ (2002) J Catal 210:1
15. Vieira R, Pham-Huu C, Keller N, Ledoux MJ (2002) Chem Commun 954
16. Vieira R, Bernhardt P, Ledoux MJ, Pham-Huu C (2005) Catal Lett 99:177
17. Vieira R, Bastos-Netto D, Ledoux MJ, Pham-Huu C (2005) Appl Catal A Gen 279:35
18. Liang CH, Tian FP, Li ZL, Wei ZB, Li C (2002) Chem Mater 15:4846
19. Li L, Wang X, Wang XD, Zhao XQ, Zheng MY, Cheng RH, Zhou LX, Zhang T (2005) Thermochim Acta 434:119
20. Volpe L, Boudart M (1985) J Solid State Chem 59:348
21. Costa PD, Lemberton JL, Potvin C, Manoli JM, Perot G, Breysse M, Djega-Mariadassou G (2001) Catal Today 65:195